LIGO SCIENTIFIC COLLABORATION
VIRGO COLLABORATION

Document Type	LIGO-T1100093-v1	February 14, 2011

Gravitational Wave Emission from Accretion Disk Instabilities – Analytic Models

Lucía Santamaría (LIGO Lab, Caltech, luciasan@caltech.edu),
Christian D. Ott (TAPIR/CaRT, Caltech, cott@tapir.caltech.edu)

Abstract

We derive the gravitational wave emission from accretion disk instabilities in long gamma-ray bursts or black-hole forming core-collapse supernovae based on simple analytic models of van Putten and Piro & Pfahl.

WWW: http://www.ligo.org/ and http://www.virgo.infn.it

Processed with LaTeX on 2011/02/14

1 Introduction

We derive analytic estimates for the gravitational wave (GW) emission from the following analytic accretion disk instability models in the context of Collapsar-type gamma-ray bursts and black-hole (BH) forming core-collapse supernovae:

- The suspended-accretion-driven disk instability proposed by van Putten [1, 2]. In this instability, turbulence in a thick accretion torus is driven by strong coupling between the torus and the ergosphere of the central BH by MHD effects. In this picture, the quadrupole components of the disk turbulence lead to GW emission that (via the strong coupling) spin down the BH. The strong coupling and the energetics of the associated GW emission proposed by van Putten are generally regarded as too optimistic (possibly by orders of magnitude). Nevertheless, we include this model, since it makes useful, falsifiable predictions.
- Fragmentation instability and inspiral as proposed by Piro & Pfahl [3]. In the Piro & Pfahl model, gravitational instability leads to fragmentation of parts of the outer accretion torus around a BH formed in the collapse of a massive star. The fragments condense to a 'blob' of neutronized matter that then spirals in due to viscosity and/or GW emission.

In the following, we work in physical units, including all relevant factors of the gravitational constant G and of the speed of light c. Accompanying this technical report are two python scripts, `vanPuttengw.py` and `pirogw.py`, that implement the models described here and provide both GW polarizations as output.

2 Suspended-Accretion Quadrupole Disk Instability

Following along the lines of van Putten's ideas, we assume a spinning Kerr BH with dimensionless Kerr spin parameter $a^\star = (c/G)J_{\rm BH}/M_{\rm BH}^2$ ($0 \leq a^\star < 1$) with an accretion disk/torus of mass $M_{\rm disk}$. The disk extends to the radius of the innermost stable orbit [4],

$$R_{\rm ISCO} = \left(\frac{G}{c^2}\right) M_{\rm BH} \left(3 + Z_2 \mp [(3 - Z_1)(3 + Z_1 + 2Z_2)]^{1/2}\right), \tag{1}$$

$$Z_1 = 1 + (1 - a^{\star 2})^{1/3} \left[(1 + a^\star)^{1/3} + (1 - a^\star)^{1/3}\right], \tag{2}$$

$$Z_2 = \left[3a^{\star 2} + Z_1^2\right]^{1/2}, \tag{3}$$

where the $\mp$ sign indicates prograde and retrograde orbits, respectively. We will assume that the binary orbits in the same direction as the BH spin and thus take the minus sign in equation 1. Disk and BH are assumed to be coupled via strong magnetic fields and MHD turbulence in the disk is assumed to be driven through this coupling. The inner disk near the ISCO is expected to be neutrino cooled and very thin. Further out, at $r_0 + R_{\rm ISCO}$ (where $r_0 = 100$ km may be reasonable), the disk is a thick torus. We assume that turbulence in the torus leads to two overdense regions (which, in itself, is unlikely, since turbulent power will cascade to small scales) with masses $M_1 = M_2 = \epsilon M_{\rm disk}$. $\epsilon \approx 0.01 - 0.5$ (the latter is very unlikely). These two 'clumps' form a 'binary' with separation $2(r_0 + R_{\rm ISCO})$ that efficiently emits GWs and would normally lose J by GW emission, leading to inspiral. The BH is located at the center of our coordinate system and each of the clumps is located at a distance $r_0 + R_{\rm ISCO}$ from the BH. Here, following van Putten, we assume that the lost energy and angular momentum is replenished by coupling to the central BH, so the BH loses J and spin energy. This leads to an incremental change of $R_{\rm ISCO}$ and, consequentially, of the binary separation $2(r_0 + R_{\rm ISCO})$.

2.1 h^{lm} and $\dot{J}$ from the Newtonian Binary Approximation

We assume that the BH angular momentum is oriented in the $+z$-direction. The two overdense regions in the torus orbit in the xy-plane with angular velocity Ω. Furthermore, we assume that the two masses are equal $M_1 = M_2 \equiv m$ and orbit in a circular orbit of radius $r_0 + R_{\rm ISCO} \equiv d$. We can compute the reduced mass quadrupole momentum of the system, defined as

$$I_{ij} = \sum_A m_A (x_{Aj} x_{Aj} - \frac{1}{3}\delta_{ij} r_A^2), \tag{4}$$

where A denotes the sum over all particles in the system. Thus

$$I_{ij} = md^2 \begin{pmatrix} 1/3 + \cos 2\Omega t & \sin 2\Omega t & 0 \\ \sin 2\Omega t & 1/3 - \cos 2\Omega t & 0 \\ 0 & 0 & -2/3 \end{pmatrix}, \tag{5}$$

$$\ddot{I}_{ij} = 4md^2\Omega^2 \begin{pmatrix} -\cos 2\Omega t & -\sin 2\Omega t & 0 \\ -\sin 2\Omega t & \cos 2\Omega t & 0 \\ 0 & 0 & 0 \end{pmatrix}, \tag{6}$$

$$\dddot{I}_{ij} = 8md^2\Omega^3 \begin{pmatrix} \sin 2\Omega t & -\cos 2\Omega t & 0 \\ -\cos 2\Omega t & \sin 2\Omega t & 0 \\ 0 & 0 & 0 \end{pmatrix}. \tag{7}$$

The gravitational wave signal emitted by the binary system and the change in angular momentum and energy are given by

$$h_{ij}^{TT} = \frac{2}{D}\frac{G}{c^4}\ddot{I}_{kl}^{TT}\bigg|_{t-r/c}, \qquad \frac{dJ_i}{dt} = -\frac{2}{5}\frac{G}{c^5}\epsilon_{ijk}\langle \ddot{I}_{jm}\dddot{I}_{mk}\rangle\bigg|_{t-r/c}, \qquad \frac{dE}{dt} = -\frac{1}{5}\langle \dddot{I}_{jk}\dddot{I}_{jk}\rangle\bigg|_{t-r/c}, \tag{8}$$

where we indicate that the right-hand side expressions are to be taken at the retarded time $t - r/c$.
Thus, in this Newtonian binary approximation we have

$$h_{ij}^{TT} = \frac{8md^2\Omega^2}{D}\frac{G}{c^4} \begin{pmatrix} \cos 2\Omega(t - r/c) & \sin 2\Omega(t - r/c) & 0 \\ \sin 2\Omega(t - r/c) & -\cos 2\Omega(t - r/c) & 0 \\ 0 & 0 & 0 \end{pmatrix}, \tag{9}$$

$$\frac{dJ_{\rm GW}}{dt} = -\frac{128}{5} m^2 d^4 \Omega^5 \frac{G}{c^5}, \tag{10}$$

$$\frac{dE_{\rm GW}}{dt} = P_{\rm GW} = -\frac{128}{5} m^2 d^4 \Omega^6 \frac{G}{c^5}. \tag{11}$$

2.2 The coupled system of Ordinary Differential Equations

We assume that the ‘binary’ stays at a fixed radius. Angular momentum J lost to GW emission is provide from the BH spin. As a consequence, the BH is spun down and $R_{\rm ISCO}$ changes. We set $\dot{J}_{\rm BH} = \dot{J}_{\rm GW}$. The change in the BH mass is

$$\dot{M}_{\rm BH} = \frac{P_{\rm GW}}{c^2}, \tag{12}$$

since the gravitational mass of the BH contains the contribution due to its rotational energy. The change in $R_{\rm ISCO}$ can then be computed by differentiating equation 1,

$$\frac{dR_{\rm ISCO}}{dt} = \dot{R}_{\rm ISCO} = \left(\frac{G}{c^2}\right)\left[\dot{M}_{\rm BH}\left(3 + Z_2 - \sqrt{(3-Z_1)(3+Z_1+2Z_2)}\right) + M_{\rm BH}\left(\dot{Z}_2 + \frac{(Z_1+Z_2)\dot{Z}_1 - (3-Z_1)\dot{Z}_2}{\sqrt{(3-Z_1)(3+Z_1+2Z_2)}}\right)\right], \tag{13}$$

where we can express Z_1, Z_2 and their derivatives as functions of $J_{\rm BH}$, $M_{\rm BH}$, $\dot{J}_{\rm BH}$, $\dot{M}_{\rm BH}$ only,

$$\dot{Z}_1 = \frac{c\left(M_{\rm BH}\dot{J}_{\rm BH} - 2J_{\rm BH}\dot{M}_{\rm BH}\right)}{3G^3M_{\rm BH}^7\left(1-a^{\star 2}\right)^{4/3}}\left[3c^2J_{\rm BH}^2\left((1+a^\star)^{2/3} - (1-a^\star)^{2/3}\right) - 2cGJ_{\rm BH}M_{\rm BH}^2\left((1+a^\star)^{2/3} + (1-a^\star)^{2/3}\right) + G^2M_{\rm BH}^4\left((1-a^\star)^{2/3} - (1+a^\star)^{2/3}\right)\right], \tag{14}$$

$$\dot{Z}_2 = \frac{3c^2J_{\rm BH}M_{\rm BH}\dot{J}_{\rm BH} - 6c^2J_{\rm BH}^2\dot{M}_{\rm BH} + G^2M_{\rm BH}^5Z_1\dot{Z}_1}{G^2M_{\rm BH}^5\sqrt{\frac{3c^2J_{\rm BH}^2}{G^2M_{\rm BH}^4} + Z_1^2}}\,. \tag{15}$$

These expressions allows us to calculate the change in $R_{\rm ISCO}$ when the mass and angular momentum of the central BH change.

2.3 Application of the coupled system

At every time t, $\ddot{I}_{ij}$ and, thus, h_{ij}^{TT} depend on (*i*) the orbital radius of the 'binary', $d = r_0 + R_{\rm ISCO}$, (*ii*) the mass m of the chunks (assumed to be constant), and (*iii*) on the angular velocity, which, according to Kepler's law, we set to

$$\Omega = \sqrt{\frac{GM}{d^3}}\,. \tag{16}$$

Let us assume that the mass of the chunks forming the 'binary' is negligible with respect to the mass of the central black hole, in which case $\Omega = \sqrt{GM_{\rm BH}/(r_0 + R_{\rm ISCO})^3}$. The coupled system of ODEs is then formed by equations 10, 12 and 13, with $d = r_0 + R_{\rm ISCO}$ and Ω as in equation 16. $P_{\rm GW}$ in equation 12 is given by equation 11. This system describes the evolution of $R_{\rm ISCO}, J_{\rm BH}$ and $M_{\rm BH}$. We integrate the coupled system of ODEs with a fourth-order Runge-Kutta integrator.

Note that once all spin has been extracted from the hole, the 'binary' will inspiral. However, we stop our integration when the BH is completelly spun down and do not calculate the subsequent chirp.

2.4 Astrophysically Meaningingful Parameters

Mass	BH of mass $M_{\rm BH} = 5 - 10\,M_\odot$
Initial BH spin	$a^\star = 0.3 - 0.95$
Fragment mass	Assume $M_{\rm disk} = 1.5M_\odot$, $m_{\rm chunk} = \epsilon M_{\rm disk}$ with $\epsilon = 0.01 - 0.2$
Const. separation of torus from ISCO	$r_0 = 100$ km
End integration	When $J_{\rm BH} = 0$ or pre-specified run time is reached

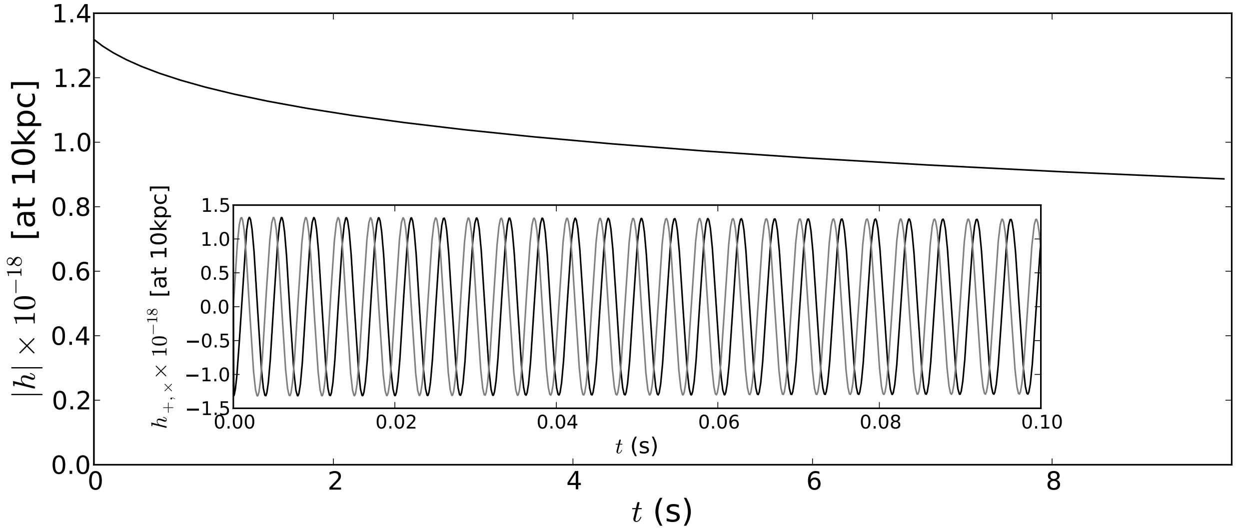

Figure 1: Waveform computed following the van Putten model. The parameters of the system are $M_{\rm BH} = 10M_\odot$, $a^\star = 0.95$, $\epsilon = 0.2$. The strain corresponds to a face-on, optimally-oriented system situated at 10 kpc. The main plot shows the absolute magnitude of the strain $|h| = \sqrt{h_+^2 + h_\times^2}$ and the inset plot shows the two polarizations zooming into the first 0.1 s of evolution.

2.5 Usage of the python script

Code usage: `$ python vanPutten.py`
The code section below `#physical parameters` allows to specify the physical parameters of the system as defined in subsection 2.4. The colatitude and azimuth of the system can be specified as well. The code section under `#parameters` allows to change the total run time (in seconds) of the integration (provided that the BH is not completely spun down, in which case the integration stops) as well as the sampling time `dt` of the output.
The script produces two output files:

- `pmvp.dat` is a diagnosis and debug output file, containing the following variables:

time	$R_{\rm ISCO}$	$J_{\rm BH}$	$M_{\rm BH}$	$a^\star$	$E_{\rm rad}$	h_+	$h_\times$

- `M*a*eps*.dat`, where the $\star$'s denote the values of the physical parameters $M_{\rm BH}$, $a^\star$ and ϵ given as input, is the production output file, containing:

time	h_+	$h_\times$

An example of the antichirp-like signal obtained for the van Putten model is shown in figure 1.

3 Torus Fragmentation Instability and Inspiral of a Single Overdense Blob

If the core-collapse supernova mechanism fails to re-energize the stalled shock (see, e.g., [5]), the protoneutron star collapses to a BH on an accretion timescale [6]. Provided sufficient angular momentum, a massive accretion disk/torus may form around the nascent stellar-mass BH. This scenario may lead to a collapsar-type gamma-ray burst or an "engine driven" supernova [7].
The inner part of the disk is geometrically thin due to efficient neutrino cooling, but outer regions are thick and may be gravitationally unstable to fragmentation at large radii. We implement the expected gravitational radiation from such a system, inspired by the discussion by Piro & Pfahl [3].

We assume a central BH of mass $M_{\rm BH}$ surrounded by a Keplerian accretion disk with orbital frequency $\Omega = (GM_{\rm BH}/r^3)^{1/2}$ and vertical scale height H. The accretion rate is $\dot{M} = 3\pi\nu\Sigma$, where Σ is the disk's surface density, $\nu = \alpha c_S H$ the usual viscosity prescription and c_S the isothermal sound speed. We assume that $H/r = \mu$ is a fixed parameter.

3.1 Gravitationaly instability and fragmentation

Gravitational instability arises when

$$Q \equiv \frac{\Omega c_S}{\pi G \Sigma} < Q_{\rm crit} \simeq 1 \ , \tag{17}$$

Under given circunstances, numerical simulations have shown that gravitational instability leads to fragmentation. As explained in [3], we can identify the quantity $(QH)^2\Sigma$ with the mass of a bound clump if cooling is rapid enough to permit collapse to high densities.

Various possible cooling mechanisms in the disk can be studied, among them radiative diffusion, neutrino cooling processes, and photodisintegration. Photodisintegration of ^{4}He will absorb sufficient energy quickly enough to allow fragmentation. Thus, it may be a very effective coolant, permitting fragmentation over a small range of radii near the location where $Q = Q_{\rm crit}$ in the perturbed disk. This allows us to estimate the mass of the bound fragment as

$$M_f \approx 0.2 \left(\frac{\eta}{0.5}\right)^3 \frac{M_{\rm BH}}{3} \ . \tag{18}$$

3.2 Migration and associated gravitational waves

If the fragment is massive enough to form a bound object and open a gap in the accretion disk, it migrates inwards, forming an inspiralling binary with the central BH. The loss of angular momentum is due to dissipation within the disk and to the emission of gravitational waves. The viscous migration happens on a the viscous timescale,

$$t_\nu \approx \frac{1}{\alpha \nu^2 \Omega} \ . \tag{19}$$

Loss of angular momentum in the form of gravitational waves causes inspiral on a time that can be estimated to first order via the quadrupole formula

$$t_{\rm GW} = \frac{5}{64\Omega}\left(\frac{G\mathcal{M}\Omega}{c^3}\right)^{-5/3} , \tag{20}$$

where $\mathcal{M}$ is the chirp mass of the system formed by BH plus fragment. The evolution of the orbit can be computed by simply solving the differential equation

$$\frac{dr}{dt} = -r\left(\frac{1}{t_{\rm GW}} + \frac{1}{t_v}\right) \tag{21}$$

The integration of equation 26 allows us to compute the chirp-like gravitational wave emission expected from this system. We make use of equation 9 where D is the distance between the central BH and the bound fragment. The ODE integration is implemented with a fourth-order Runge-Kutta integrator.

3.3 Astrophysically Meaningful Parameters

Mass	BH of mass $M_{\rm BH} = 3 - 10 M_\odot$
Viscosity	Standard value of $\alpha = 0.1$ [3]
Geometrical parameter	$\eta = 0.3 - 0.6$ [3]
Mass of the bound fragment	The approximate factor 0.2 in equation 23 can be varied from $0.2 - 0.5$
Starting Radius	Start at $r = 100 r_S$, where $r_S = \frac{GM}{c^2}$ is the gravitational radius
	End integration close to the ISCO

3.4 Usage of the python script

Code usage: `$ python pirogw.py`
The code section below `#physical parameters` allows to specify the physical parameters of the system as defined in subsection 3.7. The colatitude and azimuth of the system can be specified as well. The code section under `#parameters` allows to change the total run time (in seconds) of the integration (provided that the orbital radius is larger than $2.5 R_{\rm ISCO}$ where we take a multiple of the ISCO radius of a non-spinning black hole $R_{\rm ISCO} = 6 G M_{\rm BH}/c^2$ as a limit for the integration) as well as the sampling time `dt` of the output. The script produces two output files:

- `piro.dat` is a diagnosis and debug output file, containing the following variables:

time	r (cm)	r (r_S)	h_+	$h_\times$	Ω	t_{GW}	t_v

- `piroM*eta*fac*.dat`, where $\star$ denote the values of the physical parameters $M_{\rm BH}$, η and the factor in the RHS of equation 23 given as input, is the production output file, containing:

time	h_+	$h_\times$

An example of the chirp-like signal obtained for the Piro & Pfahl [3].
We assume a central BH of mass $M_{\rm BH}$ surrounded by a Keplerian accretion disk with orbital frequency $\Omega = (G M_{\rm BH}/r^3)^{1/2}$ and vertical scale height H. The accretion rate is $\dot{M} = 3\pi\nu\Sigma$, where Σ is the disk's surface density, $\nu = \alpha c_S H$ the usual viscosity prescription and c_S the isothermal sound speed. We assume that $H/r = \mu$ is a fixed parameter.

3.5 Gravitationaly instability and fragmentation

Gravitational instability arises when

$$Q \equiv \frac{\Omega c_S}{\pi G \Sigma} < Q_{\rm crit} \simeq 1 \ , \tag{22}$$

Under given circunstances, numerical simulations have shown that gravitational instability leads to fragmentation. As explained in [3], we can identify the quantity $(QH)^2\Sigma$ with the mass of a bound clump if cooling is rapid enough to permit collapse to high densities.
Various possible cooling mechanisms in the disk can be studied, among them radiative diffusion, neutrino cooling processes, and photodisintegration. Photodisintegration of ^{4}He will absorb sufficient energy quickly enough to allow fragmentation. Thus, it may be a very effective coolant, permitting fragmentation over a small range of radii near the location where $Q = Q_{\rm crit}$ in the perturbed disk. This allows us to estimate the mass of the bound fragment as

$$M_f \approx 0.2 \left(\frac{\eta}{0.5}\right)^3 \frac{M_{\rm BH}}{3} \ . \tag{23}$$

3.6 Migration and associated gravitational waves

If the fragment is massive enough to form a bound object and open a gap in the accretion disk, it migrates inwards, forming an inspiralling binary with the central BH. The loss of angular momentum is due to dissipation within the disk and to the emission of gravitational waves. The viscous migration happens on a the viscous timescale,

$$t_\nu \approx \frac{1}{\alpha \nu^2 \Omega} \ . \tag{24}$$

Loss of angular momentum in the form of gravitational waves causes inspiral on a time that can be estimated to first order via the quadrupole formula

$$t_{\rm GW} = \frac{5}{64\Omega} \left(\frac{G\mathcal{M}\Omega}{c^3} \right)^{-5/3} , \tag{25}$$

where $\mathcal{M}$ is the chirp mass of the system formed by BH plus fragment. The evolution of the orbit can be computed by simply solving the differential equation

$$\frac{dr}{dt} = -r \left(\frac{1}{t_{\rm GW}} + \frac{1}{t_v} \right) \tag{26}$$

The integration of equation 26 allows us to compute the chirp-like gravitational wave emission expected from this system. We make use of equation 9 where D is the distance between the central BH and the bound fragment. The ODE integration is implemented with a fourth-order Runge-Kutta integrator.

3.7 Astrophysically Meaningful Parameters

Mass	BH of mass $M_{\rm BH} = 3 - 10 M_\odot$
Viscosity	Standard value of $\alpha = 0.1$ [3]
Geometrical parameter	$\eta = 0.3 - 0.6$ [3]
Mass of the bound fragment	The approximate factor 0.2 in equation 23 can be varied from $0.2 - 0.5$
Starting Radius	Start at $r = 100 r_S$, where $r_S = \frac{GM}{c^2}$ is the gravitational radius.
	End integration close to the ISCO.

3.8 Usage of the python script

Code usage: `$ python pirogw.py`
The code section below `#physical parameters` allows to specify the physical parameters of the system as defined in subsection 3.7. The colatitude and azimuth of the system can be specified as well. The code section under `#parameters` allows to change the total run time (in seconds) of the integration (provided that the orbital radius is larger than $2.5 R_{\rm ISCO}$ where we take a multiple of the ISCO radius of a non-spinning black hole $R_{\rm ISCO} = 6GM_{\rm BH}/c^2$ as a limit for the integration) as well as the sampling time `dt` of the output. The script produces two output files:

- `piro.dat` is a diagnosis and debug output file, containing the following variables:

time	r (cm)	r (r_S)	h_+	$h_\times$	Ω	t_{GW}	t_v

- `piroM*eta*fac*.dat`, where $\star$ denote the values of the physical parameters $M_{\rm BH}$, η and the factor in the RHS of equation 23 given as input, is the production output file, containing:

time	h_+	$h_\times$

An example of the chirp-like signal obtained for the Piro & Pfahl model is shown in figure 2.

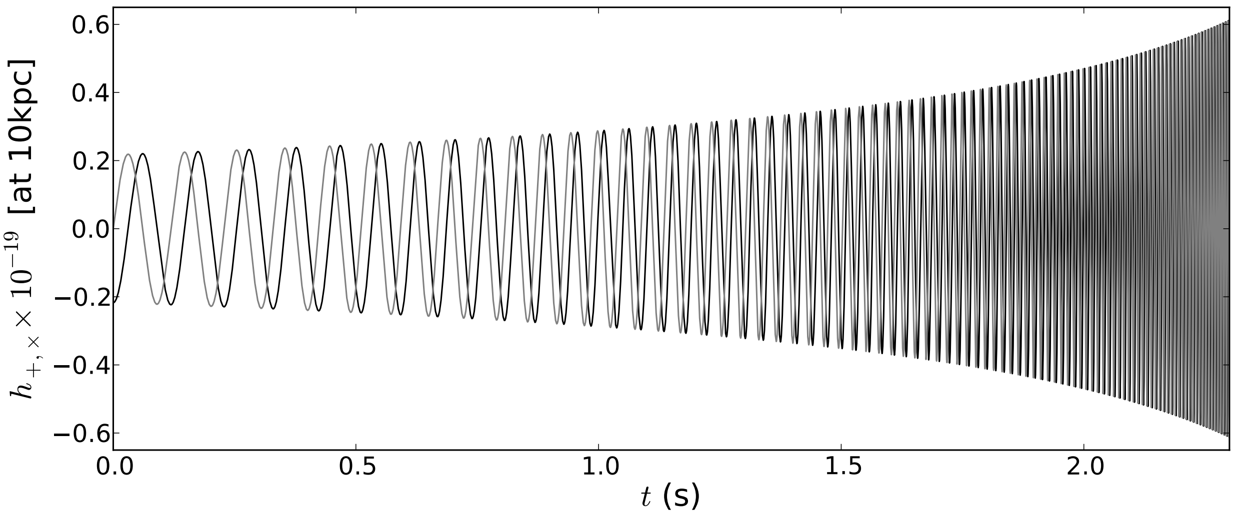

Figure 2: Waveform computed following the Piro & Pfahl model. The parameters of the system are $M_{\mathrm{BH}} = 8M_{\odot}$, $\eta = 0.3$, factor for the mass of the bound fragment = 0.2. The strain corresponds to a face-on, optimally-oriented system situated at 10 kpc.

References

[1] M. H. van Putten, A. Levinson, H. K. Lee, T. Regimbau, M. Punturo, and G. M. Harry. *Phys. Rev. D.*, **69(4)**, 044007, 2004.

[2] M. H. van Putten. *Phys. Rev. Lett.*, **87(9)**, 091101, 2001.

[3] A. L. Piro and E. Pfahl. *Astrophys. J.*, **658**, 1173–1176, 2007.

[4] J. M. Bardeen, W. H. Press, and S. A. Teukolsky. *Astrophys. J.*, **178**, 347, 1972.

[5] H.-T. Janka, K. Langanke, A. Marek, G. Martínez-Pinedo, and B. Müller. *Phys. Rep.*, **442**, 38, 2007.

[6] E. O'Connor and C. D. Ott. *Accepted for publication in the Astrophys. J., arXiv:1010.5550*, 2011.

[7] S. E. Woosley and J. S. Bloom. *Ann. Rev. Astron. Astrophys.*, **44**, 507, 2006.